Deblending of high density OBN simultaneous source acquisition offshore Indonesia

Robert To, Jain Cai, Fong Cheen Loh, Barry Hung (CGG); Simon Wolfarth (BP)*

Summary

The deblending of seismic data is highly data-dependent and can be particularly challenging when cross-talk noise is not sufficiently random. We modify the deblending approach to include both cascaded iterative signal estimation and random noise attenuation to make it more effective in this setting. Firstly we focus on retrieving the direct arrival and primary signals from shallow reflectors which are responsible for the majority of the cross-talk noise, following which we address weaker reflectors. In addition, each iteration of signal estimation is followed by three-dimensional joint low-rank and sparse inversion noise attenuation to ensure that minimal cross-talk noise enters the signal space. We illustrate the benefits of the approach on an OBN survey acquired offshore Indonesia.

Introduction

At the end of 2017 a massive OBN (3D/4C) survey was acquired offshore Indonesia using BP ISS® technology (Howe et al., 2008; Abma and Keggin, 2012; Abma et al., 2012). The survey covered an area of 730 sq.km with a trace density of approximately 5 million traces per km^2 at 4.5 km offset. In addition, very long offset data (~20 km) was also acquired for Full Waveform Inversion (FWI) studies. Data density was approximately fourteen times that of legacy OBC data (Manning et al., 2017), the volume amounting to a raw data size of ~2.5 PB. Due to time constraints, two dual-source vessels and one single source vessel were mobilized. The temporal interval between sources on the same vessel was approximately 4 seconds with a dithering time of approximately ±350 ms. The self-interference cross-talk noise (cross-talk noise generated by sources of the same vessel) proved to be the main deblending challenge.

Methodology

Suppose that the data resulting from simultaneous shooting, $\mathbf{d}$, can be represented by a series of primaries, $\mathbf{p_i}$, and corresponding cross-talk noise, $\mathbf{n_i}$:

$$\mathbf{d} = \Sigma(\mathbf{p_i} + \mathbf{n_i}) = \Sigma(\mathbf{p_i} + \Gamma\mathbf{p_i}) \quad (1)$$

where Γ is the blending operator. Here the subscript '**i**' represents different events in the seismic data. Most recent deblending algorithms (for example, Abma et al., 2010; Peng and Meng, 2016; Rohnke and Poole, 2016; Wang et al., 2016; Zhuang et al., 2017) exploit an iterative scheme to sequentially deblend primary events starting with the strongest. This is achieved through the condition that cross-talk noise is much less "predictable" compared to primaries in some domains (most notably the common receiver domain). After this step, a residual (which is the difference between the raw input and the pseudo-blended data computed from the extracted primaries) is computed and input back into the primary extraction engine for the second iteration. The process is iterated, the final result being the summation of all iterations. As the solution converges, the residual approaches zero and all the energy of the original data, $\mathbf{d}$, is said to have been attributed to a corresponding source.

Suppose that our data, $\mathbf{d}$, consists of three primary events and their corresponding cross-talk noise such that:

$$\mathbf{d} = \mathbf{p_1} + \mathbf{p_2} + \mathbf{p_3} + \mathbf{n_1} + \mathbf{n_2} + \mathbf{n_3}. \quad (2)$$

In the ideal case for the first iteration primary $\mathbf{p_1}$ is retrieved and the corresponding residual will be:

$$\mathbf{R} = \mathbf{d} - (\mathbf{p_1} + \Gamma\mathbf{p_1}) = \mathbf{d} - (\mathbf{p_1} + \mathbf{n_1}) = \mathbf{p_2} + \mathbf{p_3} + \mathbf{n_2} + \mathbf{n_3}. \quad (3)$$

Since all the unrecovered primaries are present in the residual, it is possible to retrieve all primaries from further iterations. Suppose now the retrieved signal is contaminated with cross-talk noise such that instead of $\mathbf{p_1}$ we get $\mathbf{p_1} + \mathbf{n_2}$. This is often the case when $\mathbf{n_2}$ is not sufficiently random. The corresponding residual is then:

$$\begin{aligned}\mathbf{R} &= \mathbf{d} - (\mathbf{p_1} + \mathbf{n_2} + \Gamma\mathbf{p_1} + \Gamma\mathbf{n_2}) \\ &= \mathbf{d} - (\mathbf{p_1} + \mathbf{n_2} + \mathbf{n_1} + \mathbf{p_2}) \\ &= \mathbf{p_3} + \mathbf{n_3}\end{aligned} \quad (4)$$

Now we see that $\mathbf{p_2}$ is neither in the residual nor in the retrieved primaries. This means that $\mathbf{p_2}$ has been misinterpreted as noise $\mathbf{n_2}$ and cannot be recovered regardless of how many more iterations are executed. This simple exercise illustrates that for iterative deblending algorithms, it is critical that no or minimal remnant cross-talk noise enters the primary space. Otherwise, as illustrated in Figure 1, conventional iterative deblending becomes ineffective in removing the remnant cross-talk noise.

In this work, we adopt the hybrid deblending scheme outlined by Zhuang et al., (2017). The scheme includes two main steps: (1) iterative signal extraction whose principle was outlined above; (2) after most of the signal is retrieved by signal extraction, a corresponding residual noise attenuation is computed using the Noise to Signal Ratio (NSR) as a guide. The final result is a summation of the primaries from iterative signal modelling and residual noise

10.1190/segam2018-2996789.1

attenuation. As commented by the author (Zhuang et al., 2017), this scheme has proven more effective than step (1) alone. However, as the cross-talk noise becomes less random due to denser shooting (for example, the OBN survey considered here), the hybrid deblending scheme outlined above faces challenges due to two reasons: (1) cross-talk noise separation is more challenging due to its semi-coherent nature and (2) remnant cross-talk noise enters the primary space leading to primary damage as discussed above.

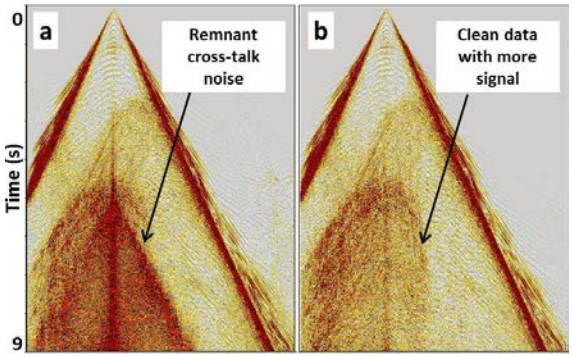

Figure 1: Comparison of results from (a) conventional iterative deblending and (b) the refined targeted deblending workflow presented in this paper (see Section Methodology for more details). (b) has less cross-talk noise and more signal recovery, especially in regions of semi coherent cross-talk noise. (Reader may refer to Figure 4a for the input)

We propose a modification of Zhuang et al., (2017), based on four considerations: (1) seismic data has an amplitude decay due to spherical divergence; (2) most of the strongest energy relates to the direct arrival and shallow reflectors whose travel time can be predicted with high accuracy based on the source-receiver offset and the speed of sound in the water layer; (3) a good inversion of the strong shallow events leads to a cleaner residual which is critical for signal extraction when cross-talk noise is less random and signal-to-noise ratio (SNR) is low; (4) additional noise attenuation can be performed after each signal modelling step without permanently damaging the data as primary damage will appear in the residual and can be recovered in later iterations.

The proposed modifications consist of two parts:

- A three-dimensional joint low-rank and sparse inversion (JLSI) noise attenuation scheme (Sternfels et al., 2015) was applied after each primary extraction step. This ensured that minimal remnant noise would enter the primary space.
- Extracted signals that are far away from the direct arrival were muted for the first few iterations until a satisfactory level of primary recovery in the shallow was reached. This ensured that no semi-coherent cross-talk noise entered the primary space in the initial iterations. After most of the energy in the shallow section had been recovered (without introducing cross-talk noise into the primary space), unrecovered primary energy in the deeper section now appeared more clearly in the residual. This allowed additional signal extraction to work more effectively in the deeper section.

A schematic display of this new flow can be seen in Figure 2 where each iteration relates to a full FK iterative deblending scheme.

Figure 3 shows a comparison between the first and the last iteration of shallow signal extraction. As more and more signal in the shallow part is recovered, the residual (Figure 3c and 3f) becomes less noisy, allowing primary selection in the region of strong, semi-coherent cross-talk noise to be more effective. The amount of random noise in Figure 3f is still noticeable as we have not completely recovered signal from shallow and deep sections. This effect can be seen in equation (3) where only a portion of primaries have been recovered. In such a case, the residual will contain both unrecovered primaries and their corresponding cross-talk noise.

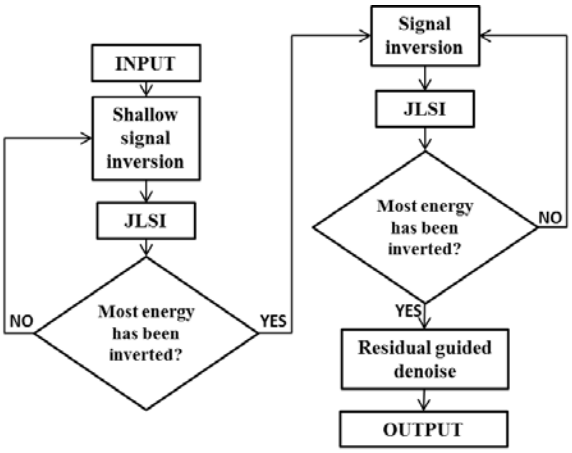

Figure 2: Schematic of the deblending flow adopted in this work. Additional JLSI noise attenuation and focus on shallow signal inversion in the initial steps are key improvements of this work.

On the other hand, the strength of the primary damage in the shallow section (as seen from the direct difference in Figure 3b and 3e) is very similar to that in the residual (Figure 3c and 3f). This shows that minimal cross-talk noise has entered into the signal space thanks to the JLSI scheme employed after each signal inversion step. At the same time such leakage can be retrieved by either signal inversion on the residual or residual guided noise attenuation.

Results and discussion

10.1190/segam2018-2996789.1

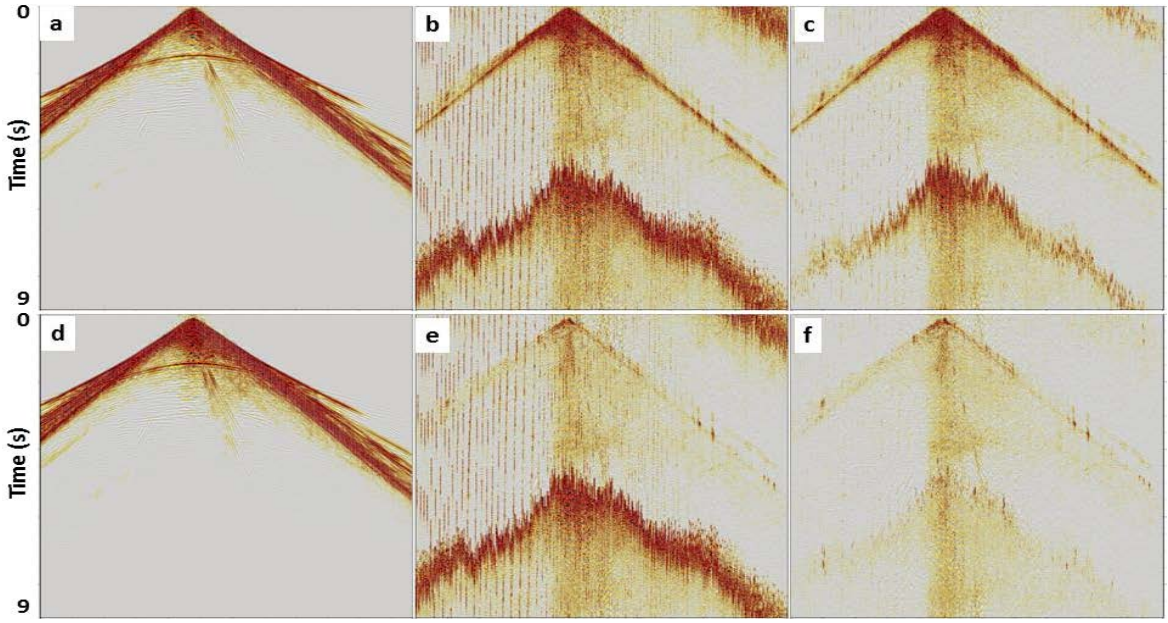

Figure 3: Comparison of the first (a, b and c) and last (d, e and f) iterations of shallow signal inversion. (a and d) are the output; (b and e) are the direct difference betewen raw input and corresponding output; (c and f) are the corresponding residual. As we progress from iteration one to three, the residual becomes cleaner, primary underlying the strong cross-talk noise becomes more obvious for subsequent signal inversion.

In Figure 4, common receiver gathers of P and Z data before deblending, after deblending, and the difference are shown. In Figures 4b and 4e we see that the cross-talk noise has been effectively attenuated. In the region of strong self-interference cross-talk noise (which can be seen from about 5 seconds to the end of the data in Figure 4a and 4d), good primary signal was recovered. No observable primary damage can be seen in the differences (Figure 4c and 4f). The good result obtained for both P and Z data validates the flow discussed in the previous section.

Another domain to QC the result is the common shot domain. In Figure 5, we show the deblended data sorted to common shot gathers for both P and Z components. From the raw input display (Figures 5a and 5d) we can see that a blend ratio of at least 4 can be identified. The output (Figure 5b and 5e) is free of any obvious cross-talk noise while the differences (Figure 5c and 5f) suggest that no obvious signal damage can be seen. The common shot results further validate the deblending flow discussed here.

Figure 6 compares Reverse Time Migration (RTM) images of the data before deblending (Figure 6a), after deblending (Figure 6b) and the differences (Figure 6c). The figure shows that the cross-talk noise in Figure 6a has been effectively attenuated after deblending, Figure 6b, while no obvious primary damage can be seen on the difference (Figure 6c). This comparison further confirms the effectiveness of the deblending approach described in this paper.

Conclusion

We have discussed an improvement to the hybrid deblending flow of Zhuang et al., (2017). The modifications consisted of (1) inclusion of JLSI noise attenuation after each signal inversion step to ensure minimal cross-talk noise enters the signal space and (2) muting off the region of severe self-interference cross-talk noise in the first few iterations until most signal in the shallow section has been achieved

These modifications are based on two aspects (beside the higher predictability of signal compared to cross-talk noise): (1) the strongest cross-talk energy relates to the direct arrival and (2) no or minimal cross-talk noise should enter into the signal space.

The flow was tested on highly dense OBN ISS® data and provided very good result for both P and Z components.

Acknowledgement

The authors would like to thank CGG and BP for the permission to publish this work.

10.1190/segam2018-2996789.1

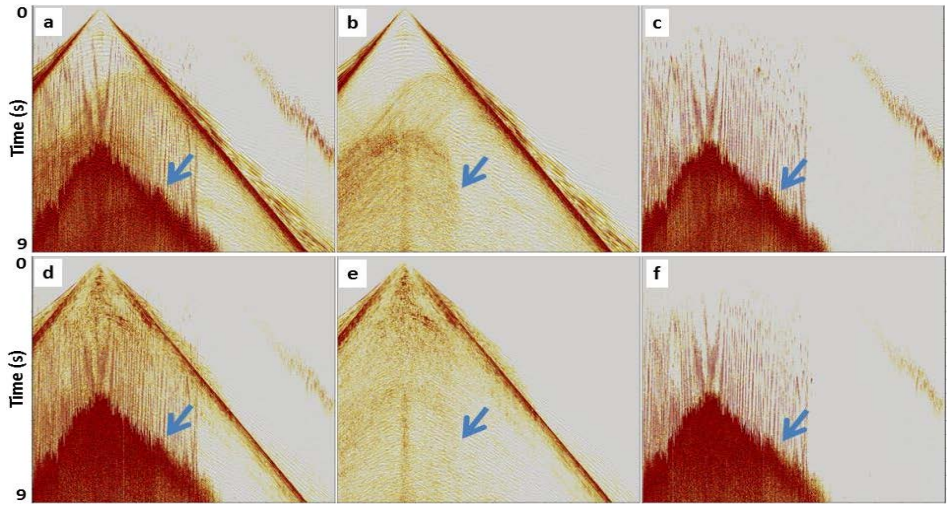

Figure 4: Common receiver gathers of P (a, b and c) and Z (d, e and f) data with (a and d) raw input before deblending; (b and e) deblending output and (c and f) difference between input and deblended data. The primary signal, especially in the self-interference region (blue arrow), has been receovered effectively while minimal primary damage can be observed on the difference.

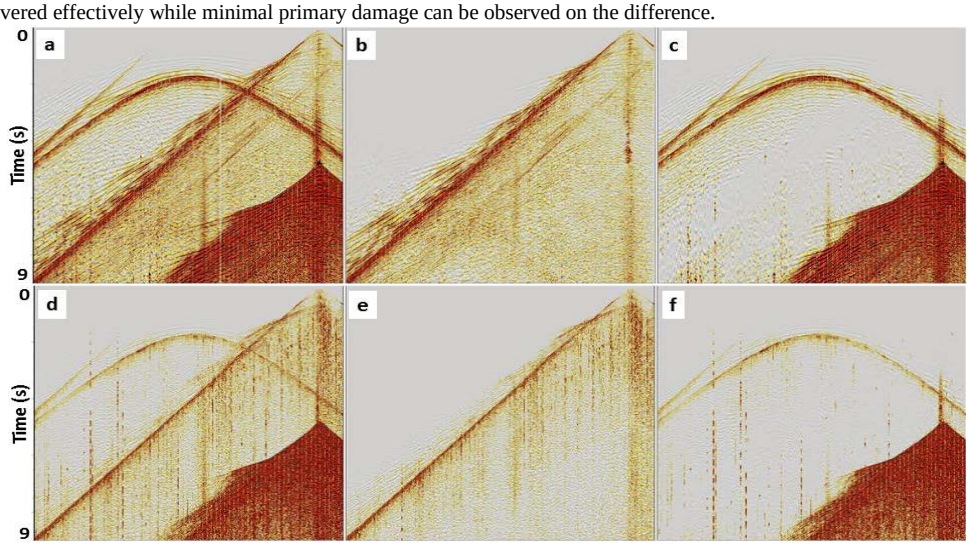

Figure 5: Common shot gathers of P (a, b and c) and Z (d, e and f) data with: (a and d) raw input before deblend; (b and e) deblend output; (c and f) difference between input and deblend. While the blending ratio went up to 4 times in this case, the deblending algorithm was able to separate the energy from different sources quite effectively.

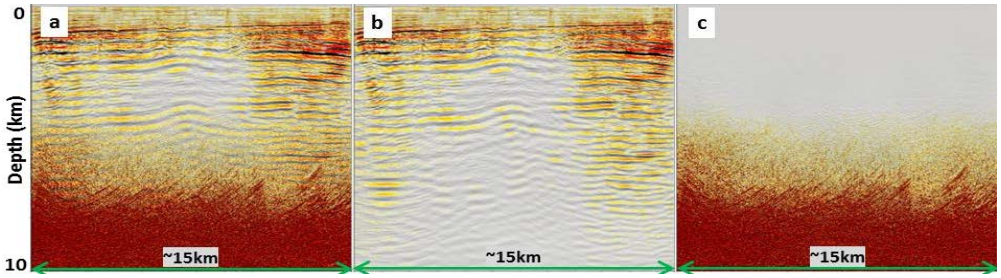

Figure 6: RTM image of the P component before deblend (a); after deblend (b) and the difference (c). Cross-talk noise was effectively removed while no obvious primary damage can be seen on the difference.

10.1190/segam2018-2996789.1

REFERENCES

Abma, R., and J. Keggin, 2012, Simultaneous shooting, today and tomorrow: 74th Annual International Meeting, SEG, Expanded Abstracts, Extended Abstracts, workshop 03, https://doi.org/10.3997/2214-4609.20149761.

Abma, R., T. Manning, M. Tanis, J. Yu, and M. Foster, 2010, High quality separation of simultaneous sources by sparse inversion: 72nd Annual International Meeting, SEG, Expanded Abstracts, Extended Abstracts, B003, https://doi.org/10.3997/2214-4609.201400611.

Abma, R., Q. Zhang, A. Arogunmati, and G. Beaudoin, 2012, An overview of BP's marine independent simultaneous source field trials: 82nd Annual International Meeting, SEG, Extended Abstracts, 1–5, https://doi.org/10.1190/segam2012-1404.1.

Howe, D., M. Foster, A. Allen, I. Jack, and B. Taylor, 2008, Independent simultaneous sweeping—A method to increase productivity of land seismic crews: 78th Annual International Meeting, SEG, Extended Abstract, 2826–2830, https://doi.org/10.1190/1.3063932.

Manning, T. A., T. Septyana, S. Putri, D. Priyambodo, F. Putro, Y. Supriatna, J. Stone, and S. Wolfarth, 2017, The role and value of geophysical studies to design and approve dense ISS® OBS survey designs—A review from Indonesia: 79th Annual International Meeting, SEG, Expanded Abstracts, Extended Abstracts, Th P8 14, https://doi.org/10.3997/2214-4609.201700780.

Peng, C., and J. Meng, 2016, Inversion-based 3D deblending of towed-streamer simultaneous source data using sparse Taup and wavelet transforms: 86th Annual International Meeting, SEG, Expanded Abstract, 4607–4611, https://doi.org/10.1190/segam2016-13866688.1.

Rohnke, J., and G. Poole, 2016, Simultaneous source separation using an annihilation filter approach: 78th Annual International Meeting, SEG, Expanded Abstracts, Extended Abstracts, We LHR2 08, https://doi.org/10.3997/2214-4609.201600953.

Sternfels, R., G. Viguier, R. Gondoin, and D. Le Meur, 2015, Multidimensional simultaneous random plus erratic noise attenuation and interpolation for seismic data by joint low-rank and sparse inversion: Geophysics, **80**, no. 6, WD129–WD141, https://doi.org/10.1190/geo2015-0066.1.

Wang, M., Z. H. Chen, C. Chen, F. C. Loh, T. Manning, and S. Wolfarth, 2016, Advanced deblending scheme for independent simultaneous source data: 25th International Geophysical Conference and Exhibition, ASEG, Extended Abstracts, 564–568, https://doi.org/10.1071/aseg2016ab158.

Zhuang, D., G. Shao, A. Khalil, B. Nolte, P. Paramo, and K. Vincent, 2017, Deblending of OBC data with dual and triple simultaneous sources offshore Trinidad: 87th Annual International Meeting, SEG, Expanded Abstract, 4914–4918, https://doi.org/10.1190/segam2017-17739616.1.